Science of the Total Environment xxx (xxxx) xxx

Contents lists available at ScienceDirect

Science of the Total Environment

journal homepage: www.elsevier.com/locate/scitotenv

Epigenetic alterations induced by aflatoxin B_1: An *in vitro* and *in vivo* approach with emphasis on enhancer of zeste homologue-2/p21 axis

Priyanka Soni [a], Md. Sajid Ghufran [a,1], Shilpa Olakkaran [b], Gurushankara Hunasanahally Puttaswamygowda [b], Govinda Rao Duddukuri [a], Santosh R. Kanade [c,*]

[a] Department of Biochemistry and Molecular Biology, School of Biological Sciences, Central University of Kerala, Tejaswini Hills, Periye, Kasargod 671316, Kerala, India
[b] Department of Zoology, School of Biological Sciences, Central University of Kerala, Tejaswini Hills, Periye, Kasargod 671316, Kerala, India
[c] Department of Plant Science, School of Life Science, University of Hyderabad, Prof. C. R. Rao Road Gachibowli, Hyderabad 500046, India

HIGHLIGHTS

- AFB_1 increases the proliferation of cells by activating Akt and its downstream signaling molecules.
- AFB_1 mediated expression of polycomb group proteins transcriptionally repress the cell cycle regulator p21.
- EZH2 mediated chromatin remodeling enhanced the p21 promoter methylation and reduced the p21 expression.
- AFB_1 upregulated the expression of E(z), Cyclin D and downregulated Dacapo expression in *Drosophila melanogaster*.

GRAPHICAL ABSTRACT

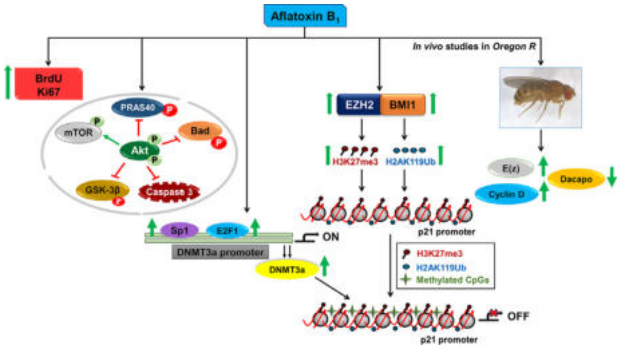

ARTICLE INFO

Article history:
Received 31 July 2020
Received in revised form 21 September 2020
Accepted 14 October 2020
Available online xxxx

Editor: Lotfi Aleya

Keywords:
Aflatoxin B_1
Polycomb group proteins
EZH2
p21
Cyclin D1
DNA methyltransferases

ABSTRACT

The potent environmental toxicant aflatoxin B_1 (AFB_1), is a group I carcinogen reported to induce the expression of many cancer associated proteins. Epigenetic alterations such as DNA methylation and histone modifications play vital role in AFB_1-mediated carcinogenesis. These epigenetic modifications may result in the recruitment of specific proteins and transcription factors to the promoter region and regulate gene expression. Here we show that AFB_1, at lower concentrations (100 and 1000 nM) induced proliferation in L-132 and HaCaT cells with activation of the Akt pathway, which ultimately steered abnormal proliferation and transmission of survival signals. We demonstrated a significant reduction in the expression of p21 with a remarkable increase in the expression of cyclin D1 that correlated with increased methylation of CpG dinucleotides in p21 proximal promoter, while cyclin D1 promoter remained unmethylated. The chromatin immunoprecipitation results revealed the enrichment of DNMT3a and H3K27me3 repressive marks on the p21 proximal promoter where EZH2 mediated H3K27me3 mark enhanced the binding of DNMT3a at the promoter and further contributed to the transcriptional inactivation. The overall study provided the novel information on the impact of AFB_1 on p21 inactivation *via* EZH2 and promoter methylation which is known to be a vital process in proliferation. Furthermore, AFB_1 induced the expression of EZH2 analogue protein E(z), cyclin D1 analogue cyclin D and decreased the expression of p21 analogue Dacapo in *Drosophila melanogaster*. Interestingly, the aggressiveness in their expression upon re-exposure in successive generations suggested first hand perspectives on multigenerational epigenetic memory.

Abbreviations: DNMTs, DNA methyltransferases; PcG, polycomb group proteins; PRC, polycomb repressive complex; EZH2, enhancer of zeste homologue 2; BMI1, B cell specific Moloney murine leukemia virus integration site 1; CDK, cyclin dependent kinase; HOX genes, Homeobox genes; E(z), enhancer of Zeste.

* Corresponding author.
E-mail address: san@uohyd.ac.in (S.R. Kanade).
[1] Present address: Department of Chemistry, Faculty of Natural and Computational Sciences, Gambella University, Gambella, P.O. Box 126, Federal Republic of Ethiopia.

https://doi.org/10.1016/j.scitotenv.2020.143175
0048-9697/

1. Introduction

A major part of the global population attains chronic exposure to several toxicants, like natural food contaminants such as mycotoxins inflicting severe health risks to the community (Dall'Asta, 2016). Aflatoxin B_1, secreted by *Aspergillus flavus* which is more prevalent in India, and *Aspergillus parasiticus*, upholds an eminent spot as the utmost potent and influential among the classes of aflatoxins (Chappell et al., 2016). The latest reports have validated that prolonged exposure to AFB_1 may adversely affect the particular epigenetic processes comprising regulation of histone modifications, gene silencing, and carcinogenesis (Bbosa et al., 2013). Plentiful of data reveals that exposure to environmental toxicants may play an inevitable role in the etiology of diverse human diseases including cancer (Herceg et al., 2013) since they impart modifications in epigenetic marks (Stein, 2012). According to these reports, a framework behind the cancer epigenetics is laid on by three specific types of genes namely, 'epigenetic mediators' which recounts the tumour progenitors; specific epigenetic modifiers' of the mediators that undergo mutation during carcinogenesis; and 'epigenetic modulators' which remain upstream of the modifiers being receptive to alterations (Feinberg et al., 2016).

Polycomb group (PcG) proteins form a major class of epigenetic regulators, which targets regulatory proteins of the cell cycle and thereby affects cellular senescence as well as cell cycle progression (Akizu et al., 2016) and may lead to the silencing of developmental regulators (Fan et al., 2011). This silencing or transcriptional suppression is brought about by polycomb repressive complexes (PRC) 1 and 2, as PRC2 initiates the silencing of genes and PRC1 stabilizes and sustains the gene expression (So et al., 2011; Aloia et al., 2013). The important protein of the polycomb repressive complex-2, called EZH2 primarily trimethylates the 27th lysine residue of the H3 histone and generates the repressive mark H3K27me3 (Akizu et al., 2016; Balasubramanian et al., 2012). Subsequently, the CBX protein of PRC1 binds to H3K27me3 and helps PRC1 to anchor the chromatin. The PRC1 subunit Ring1B ubiquitinates the lysine 119 of histone H2A (H2AK119) and in collaboration with BMI-1 increases its enzymatic activity and finally cause the suppression of gene expression (Akizu et al., 2016; Balasubramanian et al., 2012). Furthermore, it acts as a binding site for recruiting DNMTs that eventually leads to the methylation of promoters of genes (Aloia et al., 2013).

Cyclins and cyclin-dependent kinase inhibitor (CKI) proteins are among the most important cell cycle regulators. p21 is one among the cyclin dependent kinase inhibitor, plays a vital role in the cell cycle arrest. An alteration in the expression level of cell cycle regulators such as cyclin D1 and p21 is often associated with high grade tumors in multiple human cancers (Dai et al., 2017). Alterations in p21 expression are also linked with cellular senescence, aging, and tumorigenesis. Therefore, appropriate regulation of p21 expression level and activity is very important for maintaining cells in a proper differentiated state and to prevent tumorigenesis (Chen et al., 2016b).

From the past few decades, the use of model organisms had emerged as a vital tool in revealing the basis of normal cellular processes and the mechanisms underlying the onset as well as the commencement of human diseases (Gonzalez, 2013). The easy maintenance, cost efficiency, short life span of *Drosophila melanogaster* together with potent techniques for genetic manipulation, screening of genome, and epigenetic regulation makes it an inevitable model to study the characteristics of human diseases like cancer (Taylor and Tuxworth, 2019). Around 75% of *D. melanogaster* genome possess genes highly analogous to human disease and about 50% of the *Drosophila* protein sequences have particular mammalian homologues (Merinas-Amo et al., 2019). Recently emerged epigenetic research in *D. melanogaster* has grabbed prominent attention among the scientific community, unravelling the effects of posttranslational histone modifications on complex chromatin-remodeling factors and molecular machinery. For instance, the regulation of HOX genes by transcriptional modulators polycomb and trithorax group proteins during the process of embryogenesis was unveiled recently in *D. melanogaster* (Solovev et al., 2018). Another study has reported that the E(z) mediated H3K27me3 level plays a vital role in silencing several stress response genes as E(z) carry out chromatin remodeling thereby altering the gene expression at the corresponding loci (Solovev et al., 2018).

The role of AFB_1 as a carcinogen is evident however, the cellular process involved including epigenetic mechanisms that are induced by AFB_1 in carcinogenesis remain unexplored. Nevertheless, the understanding of the regulatory mechanisms involved in the maintenance of cell cycle regulators is lacking. Hence we intended to understand the mechanisms involved in the regulation of cell cycle regulator p21 along with PcG proteins. An integrative study comprising the cellular and molecular epigenetic alterations in two different model systems (*in vitro* and *in vivo*) was conducted. Study focused on the homologues of the most important epigenetic regulatory proteins such as E(z), Dacapo, and cyclin D in *Drosophila* which are solely responsible for the maintenance of the epigenetic scaffold. The *Oregon R* flies were used as a model to explore the AFB_1 mediated expression of epigenetic proteins on multigenerational epigenetic memory.

2. Material and methods

2.1. Chemicals

Fetal Bovine Serum (FBS, gamma irradiated), 1× Phosphate-buffered saline (PBS; pH: 7.4), Dulbecco's Modified Eagle's Medium (DMEM), 0.25% trypsin-0.001% EDTA (1×) solution, Antibiotic-Antimycotic solution, were purchased from Himedia Laboratories, Mumbai, India. Aflatoxin B_1 (AFB_1), Acrylamide, TEMED, *N*, *N*′-methylenebisacrylamide, Sc-79 (cat no. SML0749), Triciribine (cat no. T3830), GSK343 (cat no. SML0766), PRT4165 (cat no. SML1013) were provided by Sigma Aldrich, St. Louis, MO, USA. Horseradish peroxidase (HRP) Substrate (Clarity Western ECL) was purchased from Bio-Rad Laboratories, California, USA. Remaining chemicals and reagents were obtained from Sigma Aldrich, St. Louis, MO, USA. The ultrapure water from Milli-Q purification unit (Merck KGaA, Darmstadt, Germany) was used to prepare all the solutions and reagents used in the experiments.

2.2. In vitro culture conditions

The HaCaT (immortalized human epidermal keratinocytes) and L-132 (human lung epithelial) cells were purchased from National Centre for Cell Science (NCCS), Pune, India. The DMEM supplemented with 1× Antibiotic-Antimycotic solution and 10% Fetal Bovine Serum was used to maintain the cells in indicated culture dishes in a humidified incubator with 5% CO_2 level at 37 °C.

2.3. In vitro treatment conditions

The AFB_1 (1 mg) dissolved in 100 μl of dimethyl sulfoxide (DMSO) served as a stock. The cells were seeded into required (96 well, 60, 100 or 150 mm) dishes and later treated with AFB_1 at various doses ranging from (1 nM–100 μM). A similar amount of DMSO was used in the control.

2.4. 5′-Bromo-2′-deoxyuridine (BrdU) incorporation assay

The BrdU incorporation assay was performed in HaCaT and L-132 cells upon AFB_1 treatment. The cells were seeded in a 96 well plate at a density of 2×10^5 cells/ml overnight and exposed to varying concentrations of AFB_1 for 24 h. The proliferation of cells was assessed using a colorimetric BrdU cell proliferation kit (cat. no. ab126556) from Abcam (Cambridge, UK) following the manufacturer's instructions. Each assay was carried out in triplicates. For positive control and background reading, either wells without cells or cells untreated with BrdU were used.

2.5. Protein estimation

Bradford method (Bradford, 1976) was used to determine the protein concentration using standard bovine serum albumin solution.

2.6. PathScan® intracellular signaling array

The Cell Signaling Technology, PathScan® Intracellular Signaling Array Kit (cat. no. 7323) was used to detect the signaling nodes of cellular proteins when phosphorylated or cleaved at the specified residues. The target proteins are enlisted in Table 1. Briefly, HaCaT and L-132 cells were plated in 60 mm culture dishes followed by treatment of 1000 nM AFB_1 for 24 h. Total cellular extracts at two different dilutions (0.5 and 1.0 μg/μl) were prepared using lysis buffer provided in the array kit, and then incubated overnight onto the membrane of array-slide at 4 °C under shaking condition. After overnight incubation the array-slide was washed with 1× wash buffer followed by incubation with 1× Detection Antibody Cocktail for 1 h at room temperature. In the next step, the slide was washed again and incubated with Streptavidin-conjugated 1× HRP and visualization was performed using LumiGlo and peroxide reagent. The signal from the array-slide was detected by the Bio-Rad Versadoc Imaging System. The intensity of the signal was quantified using the Image Lab software (Bio-Rad).

2.7. Activation and inhibition study

For activation/inhibition assay, cells were first incubated with Akt activator (10 μM Sc-79) or Akt inhibitor (5 μM Triciribine) or EZH2 inhibitor (3 nM GSK343) or BMI1/RNF2 inhibitor (20 μM PRT4165) and then treated with AFB_1 (1000 nM) for 24 h. Cells without treatment were used as control.

2.8. RNA isolation, cDNA synthesis and quantitative real-time PCR

The HaCaT and L-132 cells were incubated with varying concentrations (10 nM–1000 nM) of AFB_1 in the indicated culture media without serum for 6, 12, or 24 h. After indicated time of incubation, total RNA from the treated or untreated cells for each group was isolated by the TRIzol method (Invitrogen, San Diego, CA). The cDNA was prepared using, Applied Biosystems' cDNA synthesis kit. The quantitative real-time polymerase chain reaction (qRT-PCR) analysis of genes including glyceraldehyde-3-phosphate dehydrogenase (GAPDH), Ki67, cyclin A2, cyclin B1, cyclin D1, cyclin E1, p21, cyclin D, Dacapo and E(z) were conducted with transcript-specific primers provided in Table 2, using the LightCycler 480 instrument II (Roche Molecular Systems, Pleasanton, California). The qRT-PCR reactions were carried in triplicates with LightCycler 480 SYBR Green I Master mix. A non-template negative control was run alongside the samples. The GAPDH level was used to calculate the ΔCt values for all genes. The fold change in the treatment group was calculated using the double delta CT (ΔΔCt) values normalized against GAPDH expression level in the control or untreated group. All primers were more than 95% specific and efficient as confirmed by the melting curve and sequence blast analysis.

Table 1
List of signaling proteins and their modifications upon exposure to AFB_1.

Target	Phosphorylation site	Modification
Akt	Ser 473	Phosphorylation
mTOR	Ser 2448	Phosphorylation
PRAS40	Thr 246	Phosphorylation
Bad	Ser 112	Phosphorylation
GSK-3β	Ser 9	Phosphorylation
Caspase 3	Asp 175	Cleavage
ERK1/2	Thr 202/Tyr 204	Phosphorylation
p38	Thr 180/Tyr 182	Phosphorylation

2.9. Immunoprecipitation

For performing immunoprecipitation, cells were incubated with 1000 nM AFB_1 for 24 h. Afterward, cells were washed with phosphate buffer saline and lysed in Radioimmunoprecipitation assay buffer (RIPA buffer) (Cell Signaling Technology) comprising protease inhibitor cocktail (Thermo Scientific, Waltham, Massachusetts, United States) and subjected to centrifugation for 10 min with a speed of 10,000 rpm at 4 °C. The supernatant was then incubated with specific primary antibody (Table S1) or rabbit IgG as control and prewashed protein A-agarose beads overnight at 4 °C. The nonspecific proteins were removed by washing the immunocomplexes with RIPA buffer. After the final washing step, the beads were collected, boiled in SDS-PAGE sample buffer, and cleared by centrifugation, and the supernatant containing immunoprecipitated proteins were subjected to SDS-PAGE followed by Western blotting.

2.10. Western blot analysis

The cells were treated with varying doses of AFB_1 for the indicated time. Afterward, cells were washed with phosphate buffer saline, following with lysis using RIPA buffer comprising protease inhibitor cocktail, 1 mM Dithiothreitol (DTT) and 1 mM Phenylmethanesulfonyl fluoride (PMSF) (Thermo Scientific) at 4 °C. The cellular lysate was subjected for centrifugation at 10,000 rpm for 10 min at 4 °C. Using Bradford's protocol, protein concentration was determined and equal concentration of proteins were loaded on SDS-PAGE (10 or 12%) following the method of Laemmli (Laemmli, 1970) further followed by transfer onto PVDF membranes for immunoblot. Membrane was blocked with skimmed milk (prepared in Tris-buffer saline containing Tween 20) and incubated overnight with appropriate primary antibody at dilutions mentioned in supplementary Table S1 against the target proteins at 4 °C. The HRP-conjugated secondary anti-rabbit or anti-mouse antibody at 1:10000 dilution was used. The clarity western blot developing solutions from Bio-Rad was used and band intensity was measured using the Bio-Rad Versadoc Imaging System and Image Lab software. The β-actin served as loading control.

2.11. Methylation specific PCR

The validation of methylation of the CpG islands in the p21 promoter was carried out using methylation specific PCR (MSP). For that, the cells were incubated with 1000 nM dose of AFB_1 for 24 h. Post treatment, the bisulfite conversion of the isolated genomic DNA was performed by EpiTect LyseAll Bisulfite kit (Cat. no. 59864; Qiagen, Hilden, Germany) as per manufacturer's protocol. Afterward, the bisulfite converted DNA was used for amplification in methylation specific PCR. The methylated and unmethylated sets of primers used for p21 promoter analysis were designed by the MethPrimer program and primer sequences are

Table 2
Primer sequences used for qPCR analysis.

Gene	Forward primer (5′-3′)	Reverse primer (5′-3′)
For *in vitro* studies		
GAPDH	TCCACTGGCGTCTTCACC	GGCAGAGATGATGACCCTTT
Ki67	CCACACTGTGTCGTCGTTTG	CCGTGCGCTTATCCATTCA
p21	AAGACCATGTGGACCTGTCACTGT	AGGGCTTCCTCTTGGAGAAGATCA
Cyclin A2	CTGCTGCTATGCTGTTAGCC	TGTTGGAGCAGCTAAGTCAAAA
Cyclin B1	GACAACTTGAGGAAGAGCAAGC	ATGGTCTCCTGCAACAACCT
Cyclin D1	CTGGAGGTCTGCGAGGAA	GGGGATGGTCTCCTTCATCT
Cyclin E1	TTTGCAGGATCCAGATGAAGA	CACAGACTGCATTATTGTCCCAAG
For *in vivo* studies		
GAPDH	CCCAATGTCTCCGTTGTGGA	TGGGTGTCGCTGAAGAAGTC
Cyclin D	CGCAGCATCTCTCGCAAATC	GACCCAAAGTTGTGCTGCTG
Dacapo	CCCGAGTCCTGAATCCTGTG	TGGAGCTACCGAAGAGGTCA
E(z)	TCCATGCGACATGAACTGCT	GATTCTGGCAATCGCTGCTG

Table 3
Primer sequences used for Methylation specific PCR.

Promoter	Forward primer (5′-3′)	Reverse primer (5′-3′)	CGI size	Product length
p21 (M)	AGTTAGGAGTTTGGGTTTCG	ACAACTACTCACACCTCAACTAACG	176	145
p21 (U)	AGTTAGGAGTTTGGGTTTTG	AACTACTCACACCTCAACTAACACA		143
Cyclin D1 (M)	AAAATCGGATTATAGGGGTAATTTC	TATTAAACAAAAATCAAAACCCGAC	249	175
Cyclin D1 (U)	GAAAATTGGATTATAGGGGTAATTTT	TATTAAACAAAAATCAAAACCCAAC		176

M: Methylation specific primer; U: Unmethylation specific primer.

supplied in Table 3. In this experiment, EpiTect PCR control DNA set from Qiagen was used. It comprises bisulfite converted unmethylated and methylated and also unconverted unmethylated DNA as positive control and negative control. The specificity of the amplified PCR products was affirmed by 1% agarose gel electrophoresis. The intensity of the bands on the gel was quantified by densitometry using the Image Lab software (Bio-Rad). The experiment was repeated three times. The percentage of DNA methylated in every group was calculated as methylation intensity / (methylation intensity + unmethylation intensity) × 100.

2.12. Chromatin immunoprecipitation-qPCR (ChIP-qPCR)

We followed the protocol developed by Nelson et al. (2006), with minor modifications. Cells were incubated with 1000 nM of AFB_1 for 24 h of exposure and later chromatin was prepared as follows. The cells were cross-linked and quenched with formaldehyde (1%) and glycine (125 mM) respectively and harvested post lysing with IP buffer [NP-40 (0.5% *v*/*v*), 50 mM Tris-HCl (pH 7.5), Triton X-100 (1.0% *v*/*v*), 5 mM EDTA, 150 mM NaCl] comprising cocktail of protease inhibitors (Thermo Scientific). Chromatin shearing was performed mechanically by sonication on ice to generate DNA fragments of 0.5–1 kb in size. The lysates were then cleared by centrifugation and from the supernatant retained; aliquots of sheared chromatin were made (to be used as a control for the amount of input DNA; for isolation of total DNA and to be used with multiple antibodies). The prepared chromatin was then subjected to immunoprecipitation with specific ChIP validated antibodies H3K27me3, DNMT3a, or control IgG (mock) coupled to protein A-agarose beads and incubated overnight at 4 °C with constant rotation. After clearing the chromatin with thorough washes, the DNA was purified using the QIAquick PCR Purification Kit (Cat. no. 28106; Qiagen, Hilden, Germany) and subjected to real-time qPCR analysis with Light Cycler 480 SYBR Green I Master mix in a LightCycler 480 instrument II (Roche Molecular Systems, Pleasanton, California). The target specific primers used to amplify segments of p21 promoter are enlisted in Table 4. The qPCR products were later resolved in agarose gel electrophoresis. The experiment was repeated at least 3 times.

Table 4
Primer sequences used for ChIP-qPCR.

p21 promoter region (relative to TSS)	Forward primer (5′-3′)	Reverse primer (5′-3′)	Amplicon size
Region 1 (−594 to −504)	CTGGCCTCAAGATG CTTTGT	TCACCTCTATTCCCAC TGATCC	91
Region 2 (−484 to −378)	AAATTGCAGAGAGG TGCATCGTT	CACTCTGGCAGGCA AGGATTTA	107
Region 3 (−306 to −216)	TCCAAGTAAAAAAA GCCAGATT	CTTCCCTCCTCCCCCA GTCCCT	91
Region 4 (−119 to −17)	CCCGGGGAGGGCGG TCCCGGGC	AGCTCAGCGCGGCC CTGATA	103
DNMT3a promoter			
Region 1 (−821 to −676)	AGCCTGCGGGACGG CCAGGA	CTGCCTCAGCACTG GGGCTGGGG	146
Region 2 (−406 to −253)	CGGTCTGGGCGGTG CGGGGTC	GCGCCGACTGGGGG GCCCCGGG	154
Region 3 (−174 to +17)	GCGGAGGCCTGGGC CCGCGGGC	TCTCGCCGCCGCCG CCGCCCGCG	158

2.13. Drosophila melanogaster culture

Wild type *Drosophila melanogaster* strain *Oregon-R*, received as a generous gift from Dr. H.P. Gurushankara, Department of Zoology, Central University of Kerala, Periye, was used in the study. The isogenic fly line of *Oregon R* strains was grown in culture bottles (150 mL) at the aforementioned Department, following the standard culture conditions at 24 ± 1 °C, with 60–70% relative humidity, 12 h/12 h light/dark, photoperiod on a regular wheat cream-agar medium (25–30 ml) containing yeast granules that served as a protein source up to 10–14 days. Both larval, as well as the adult numbers, were maintained to moderate densities with 50–100 larvae per bottle.

2.14. In vivo treatment conditions

The stock solutions of AFB_1 as prepared in Section 2.5 was used for treatment. Aflatoxin B_1 was added to freshly prepared standard wheat cream-agar medium to make desired concentrations (0–30 μM) and then mixed, poured to the culture bottles or vials, stoppered with foam plugs and frozen until further used. During the experiments, the vials were warmed to room temperature before use. All the experiments were performed at 24 ± 1 °C. The DMSO and diet media without AFB_1 was used as the experimental and negative control respectively. For epigenetic regulators analysis, the eggs were reared and cultured in media containing AFB_1. Once the F1 generation flies emerged, they were used for gene expression analysis as well as for recovery in normal media without AFB_1. The experiments were repeated in similar way up to F4 generation along with the generation wise recovery of flies in untreated media.

2.15. Feeding assay

The protocol developed by Lee et al. (2010) was followed with some variations to perform the feeding assay. Briefly, around 30 third instar larvae were reared in culture vials containing standard food media having orange-red synthetic food dye and 0–12 μM dose of AFB_1. After four hours of feeding, the larvae were washed with PBS and homogenized using distilled water. The homogenized solution was then centrifuged at 12,000*g* for 8 min and the supernatant was diluted 100 times. The absorbance of diluted homogenate was measured using a T60U UV-VIS spectrophotometer (PG Instruments Limited, Leicestershire, United Kingdom) at 595 nm. The assay was performed in triplicates for three times.

2.16. Lethal concentration analysis for Oregon R flies

The broadly employed Delcour's method (Delcour, 1969) was followed to generate synchronized young as well as adult flies. The *Oregon R* isogenic flies were reared in standard *Drosophila* wheat cream-agar medium and allowed to mate and lay eggs at Delcour medium (comprising agar, ethyl alcohol, acetic acid) for 12 h. The eggs collected were used for 50% lethal concentration analysis (Melone and Chinnici, 1986). Twenty eggs were collected and transferred to respective culture vials containing varying concentrations of AFB_1 treated media ranging from 0 to 30 μM. The eggs were allowed to develop on food comprising

respective concentrations of AFB_1. In each experimental group, the number of flies that emerged from these vials was accounted every day from the day of eclosion till the day of emergence which finally revealed the percentage survival of viable flies emerged post treatment with AFB_1. The experiment was conducted in triplicates for at least three times.

2.17. Locomotory behavioural assay

Flies were subjected to locomotory behavioural assay or negative geotaxis assay (Bartholomew et al., 2015; Taylor and Tuxworth, 2019) wherein the ability of AFB_1 treated and untreated flies to climb vertically were recorded. Fly groups treated with either single or multiple exposure at doses (0.75 and 1.5 μM) of AFB_1 were later transferred to culture vials with standard wheat-cream agar medium to allow the flies for recovery in a normal medium. This was followed by monitoring the climbing response in a 24 h interval to analyse the ability of flies to recover from the AFB_1 induced locomotory defects (if any). In all groups, 30 flies (ten flies each in three replicates) per sex were tested. Vertical glass cylinders/columns were marked with an 8 cm line, from the base and used as the climbing apparatus. To accustom laboratory temperature and humidity the flies were brought to room temperature one hour prior to the climbing assay. Flies were carefully transferred to new food vials before the assay since it helps in reducing wet food which may inhibit their climbing ability. The flies were then released into the vertical glass cylinders/columns and tapped to the bottom. They were allowed 30 s to climb past a line marked 8 cm from the bottom of the climbing apparatus. The number of flies above the 8 cm mark was counted and determined manually from recordings. At every 25 s interval tap was repeated two times.

2.18. Statistical analysis

Post hoc test for the analysis of variance (ANOVA) was used to present the statistical significance and threshold value of $p < 0.05$ was considered to mark the statistically significant difference, where (*), (**), and (***) indicate $p < 0.05$, $p < 0.01$ and $p < 0.001$ respectively. All experiments were conducted at thrice in triplicates and the representative result was presented as mean ± S.D. in the statistical analysis.

3. Results

3.1. Effect of AFB_1 on cell proliferation

The effect of AFB_1 on cell proliferation was determined by performing BrdU incorporation assay and analysis of Ki67 mRNA expression. A significant increase in BrdU incorporation was witnessed in both L-132 and HaCaT cells with the highest incorporation at 1000 nM of AFB_1 with respect to the control cells (Fig. 1A). To estimate the proliferation index, we examined the quantitative mRNA expression of Ki67 post 12 as well as 24 h of treatment with AFB_1 in L-132 and HaCaT cells. The results showed a significant increment in expression levels of the Ki67 gene in a time and dose dependant manner in both cell lines (Fig. 1B; Fig S1). The L-132 cells exhibited three and seven times upsurge ($p < 0.01$ and $p < 0.001$) in Ki67 mRNA expression post 12 and 24 h (exposure to 1000 nM of AFB_1), respectively. In the case of HaCaT cells, we noticed an increment ($p < 0.05$) in the expression post 12 h of treatment with 100 and 1000 nM AFB_1. Interestingly, 24 h of exposure to 100 and 1000 nM of AFB_1, led to a noteworthy 5 ($p < 0.001$) and 8 fold ($p < 0.001$) enhancement in Ki67 mRNA abundance (Fig. 1B). These results once again avowed the AFB_1 mediated cell proliferation in L-132 and HaCaT cells.

3.2. Effect of AFB_1 on intracellular signaling molecules

The cell signaling array experiment was performed to investigate intracellular signaling pathways that get activated upon AFB_1 treatment and results are summarized in the Table 1. It demonstrated that the phosphorylation level of protein kinase B (Akt), mammalian target of rapamycin (mTOR), extracellular-signal-regulated kinase (ERK1/2), Bcl-2 associated agonist of cell death (Bad), proline-rich Akt substrate of 40 kDa (PRAS40) and glycogen synthase kinase 3 beta (GSK-3β) were increased with caspase-3 cleavage and a decreased phosphorylation of p38 at two different dilutions (0.5 and 1.0 μg/μl) in HaCaT and L-132 cells (Fig. 2A–H). There was a significant activation of Akt ($p < 0.05$) as it get phosphorylated at Ser 473 residue post AFB_1 exposure along with mTOR activation *via* increased phosphorylation ($p < 0.05$) at Ser 2448. The AFB_1 treatment paved the way towards an increment in phosphorylation at Thr 246 ($p < 0.001$) and Ser 9 ($p < 0.001$) residues and further inhibition of PRAS40 and GSK-3β respectively which promote the cell survival. A significant decrease in

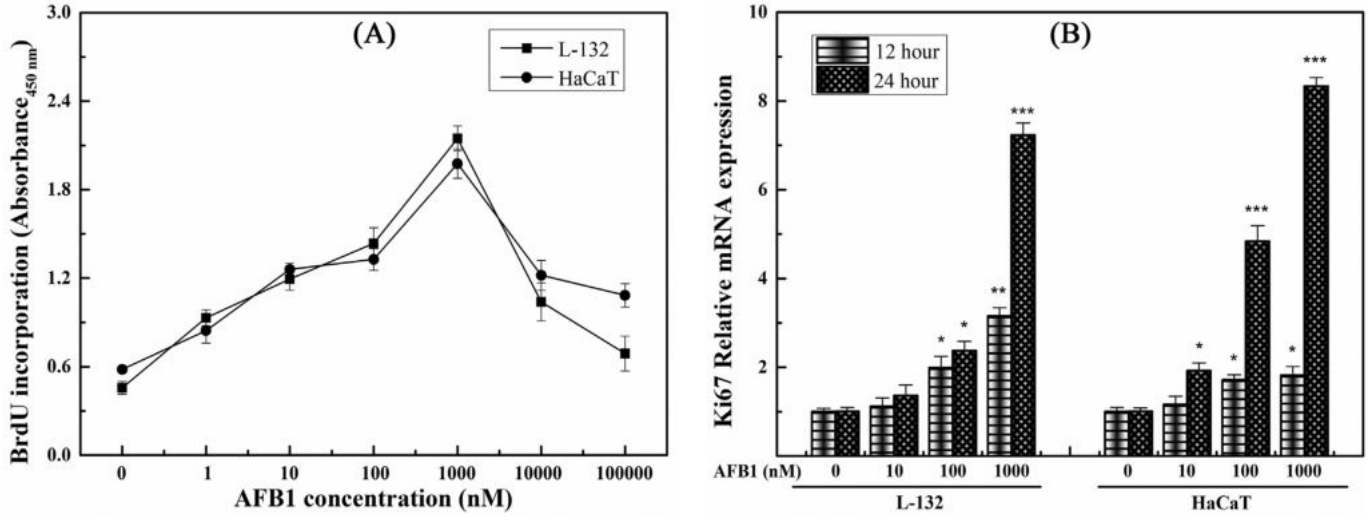

Fig. 1. Effect of AFB_1 on cell proliferation in L-132 and HaCaT cells. **(A)** Assessment of cell proliferation using the BrdU ELISA assay. The assay was performed as mentioned in the methods. Cells grown at 0.1% (*v*/*v*) of DMSO were used as an internal control. **(B)** Quantification of Ki67 mRNA expression after incubation with indicated concentrations of AFB_1 for indicated time period by real-time qPCR analysis. The data were normalized according to the ΔΔCt method against reference gene (GAPDH) expression level in the control or untreated group. The data shown statistically represents a mean ± S.D. of triplicates which provided similar results. The statistically significant difference at $p < 0.05$, $p < 0.01$ and $p < 0.001$ level denoted as *, ** and *** respectively against control group.

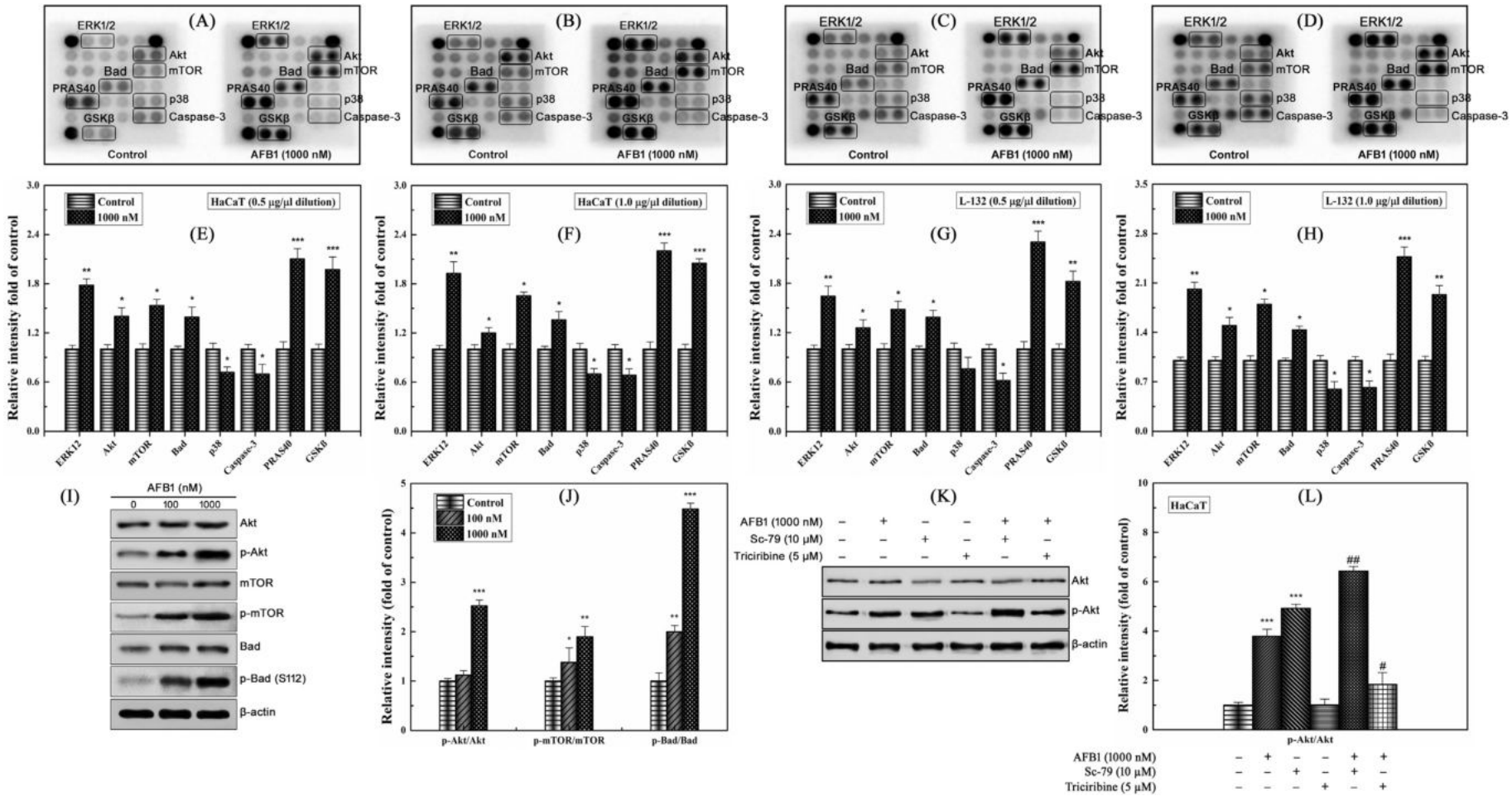

Fig. 2. PathScan® Intracellular Signaling Array in human epithelial cells. The results revealing various phosphorylated signaling nodes in the absence or presence of AFB_1 at 1000 nM concentration in **(A, B)** HaCaT **(C, D)** L-132 cells. The phosphorylation status of 18 important signaling proteins were monitored utilizing PathScan® Intracellular Signaling Array kit from CST. **(E, F, G, H)** The histogram represents dots intensities with relation to control. **(I)** Aflatoxin B_1 mediated activation of Akt pathway members in HaCaT cells. Post incubation of cells with AFB_1 at mentioned doses for 24 h, the cellular lysate (20 microgram) was subjected to immunoblot analysis with Akt, p-Akt, mTOR, p-mTOR, Bad, and p-Bad antibodies as described in the Material and methods section (Table S1). The β-actin served as the loading control. Cells grown at 0.1% (*v*/*v*) of DMSO were used as an internal control. **(J, L)** The graph represents fold intensities of band related with the control. **(K)** Effect of Akt activator and inhibitor on AFB_1-mediated expression of Akt and p-Akt. The cells were first treated with 10 μM of Akt activator (Sc-79), 5 μM of Akt inhibitor (Triciribine), for one hour and afterward, treated with AFB_1 at a concentration of 1000 nM. The cell lysates were prepared to detect the level of Akt and p-Akt protein. The β-actin served as the loading control. The data statistically represents a mean ± S.D. of triplicates which provided similar results. The statistically significant differences at $p < 0.05$, $p < 0.01$ and $p < 0.001$ level denoted as *, ** and *** respectively against control group, whereas # and ## indicate significant differences at $p < 0.05$ and $p < 0.01$ level *versus* 1000 nM AFB_1.

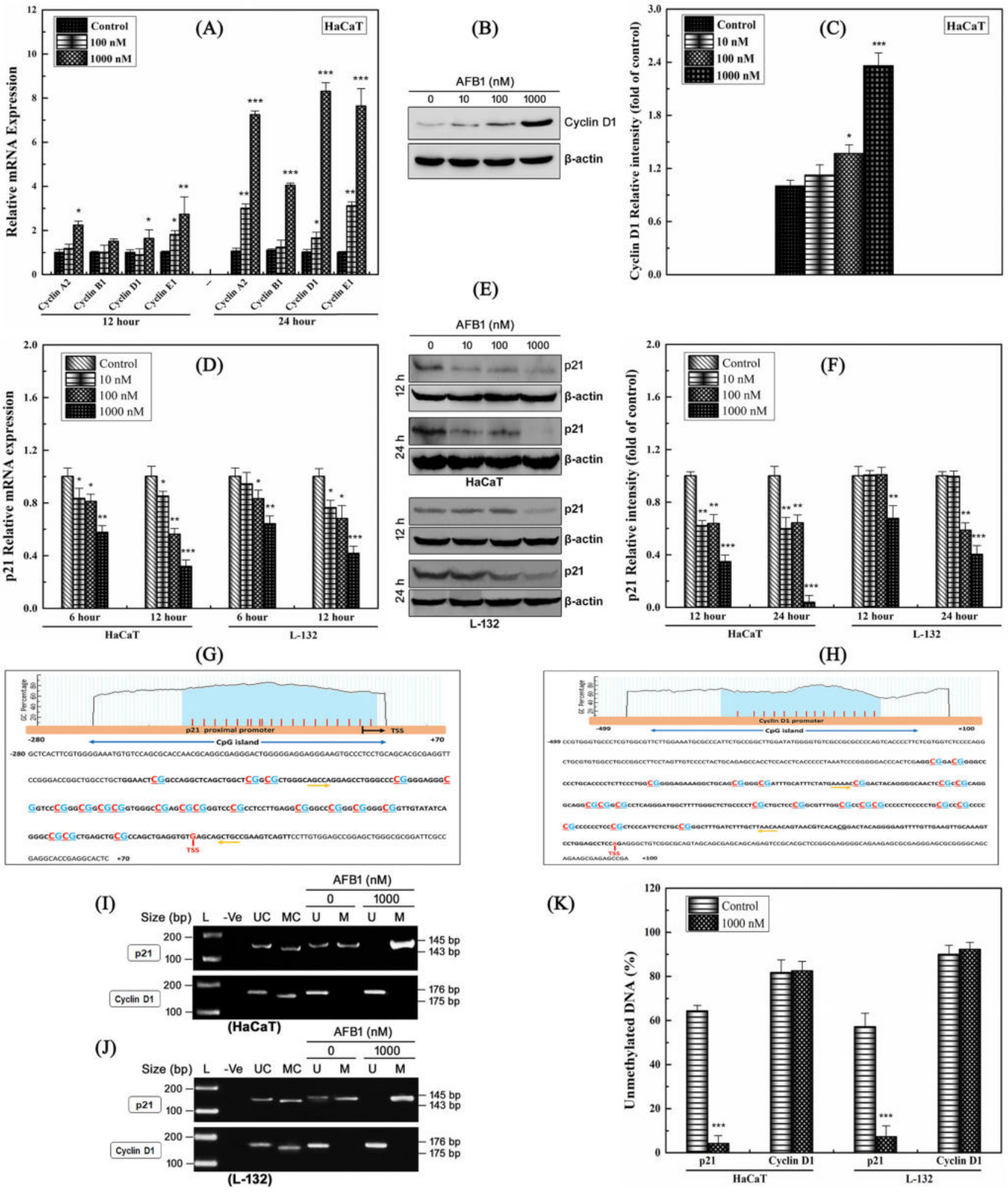

Fig. 3. Effect of AFB_1 on cell cycle regulators. **(A, D)** Time and dose dependent gene expression of cyclins and p21. Post incubation with indicated concentrations of AFB_1 for indicated time period, the relative expression of cyclin A2, B1, D1, E1 and p21 mRNA were quantified by real-time qPCR analysis. The data were normalized according to the ΔΔCt method against reference gene (GAPDH) expression level in the control or untreated group. **(B, E)** The protein abundance of cyclin D1 and p21 post 12 or 24 h of treatment with AFB_1 at 10, 100 and 1000 nM concentrations. Total protein (20 microgram) was subjected to immunoblot analysis to detect expression level of cyclin D1 and p21 protein. The β-actin served as the loading control. Cells grown at 0.1% (*v*/*v*) of DMSO were used as an internal control. **(C, F)** The graph represents fold intensities of band related with the control. **(G, H)** Schematic representation of the CpG islands in the p21 and cyclin D1 promoter as predicted by MethPrimer. **(I, J)** Agarose gel analysis of the MSP products of the p21 and cyclin D1 promoter obtained after AFB_1 exposure in HaCaT and L-132 cells. L = DNA marker; Negative control: No Genomic DNA; UC: Unmethylated control DNA; MC: Methylated control DNA; U: PCR product obtained using pairs of unmethylated-specific primer; M: PCR product obtained with pairs of methylation-specific primer. **(K)** The histogram represents the intensity level of the unmethylated DNA percentage. The data statistically represents a mean ± S.D. of triplicates which provided similar results. The statistically significant difference at $p < 0.05$, $p < 0.01$ and $p < 0.001$ level denoted as *, ** and *** respectively against control group.

the endoproteolytic cleavage of crucial mediator of apoptosis, caspase-3 ($p < 0.05$) at Asp175 leading to its inactivation and inhibit the pro apoptotic activity. A remarkable increase in phosphorylation of ERK1/2 ($p < 0.01$) at Thr 202/Tyr 204, and decrease in p38 phosphorylation ($p < 0.05$) at Thr 180/Tyr182 was noticed. In summary, AFB_1 exposure resulted in the activation of the central Akt proliferative pathway by either inhibiting or activating its downstream targets *via* phosphorylation of specific targets (Fig. 2A–H). The results demonstrated that the signaling molecules which were activated may have a direct role in the activation of a cascade of cellular events related to the cycle progression and survival.

3.3. Activation of the Akt pathway and its downstream targets

The cell signaling array results were further validated by analysing the downstream targets of Akt pathway independently post 24 h of treatment with AFB_1 in HaCaT cells. The phosphorylation of Akt, mTOR, and Bad remarkably increased with the highest expression ($p < 0.01$) at 1000 nM of AFB_1 (Fig. 2I, J). To confirm the AFB_1 mediated activation of Akt, the HaCaT cells were treated with potent Akt activator (Sc-79) and Akt inhibitor (Triciribine) in presence and absence of AFB_1. The result suggested that treatment with either AFB_1 (1000 nM) or Sc-79 (10 μM) significantly increased the phosphorylation of Akt by ~4 and ~5 fold respectively, whereas Sc-79 along with AFB_1 posed remarkable increase in the Akt phosphorylation (Fig. 2K, L). However, AFB_1 mediated activation of Akt declined by ~4 fold in the presence of Triciribine (5 μM) (Fig. 2K, L).

3.4. Effect of AFB_1 on cyclin D1 and p21 (CIP1/WAF1)

As AFB_1 has a role in cell proliferation and pro survival signaling, next we analysed the level of cyclins and cyclin-dependent kinase inhibitor (CKI) upon treatment with different doses of AFB_1. The results showed that, post 24 h of exposure to 1000 nM AFB_1 in HaCaT cells imparted a significant ($p < 0.001$) increase in the gene expression level of cyclin A2, cyclin B1, cyclin D1 and cyclin E1 (Fig. 3A) and cyclin D1 protein ($p < 0.001$, Fig. 3B, C).

Among the CKI, the mRNA and protein expression of p21 (Cip1/Waf1) was analysed upon AFB_1 exposure in HaCaT and L-132 cells. Interestingly, the expression of p21 mRNA and protein reduced in a dose and time dependent manner (Fig. 3D, E, F). Notably, the protein expression of p21 almost declined completely post 24 h ($p < 0.001$) when exposed to 1000 nM of AFB_1, in contrast, with the increased expression of cyclin D1.

3.5. AFB_1 exposure imparts repressive methylation marks on the p21 (CIP1/WAF1) promoter but not cyclin D1

Although, both the p21 and cyclin D1 promoters potentially harbour CpG islands (Fig. 3G, H), AFB_1 selectively suppressed p21 expression while cyclin D1 was overexpressed. Therefore, we analysed the methylation status of the CpG islands in both p21 (Waf1/Cip1) and cyclin D1 promoter by methylation specific PCR in HaCaT and L-132 cells. As shown in Fig. 3I, J and K, AFB_1 significantly reduced the percentage of unmethylated DNA or increased the percentage of methylated DNA in the p21 (CIP1/WAF1) promoter (−280/+70). Interestingly, the CpG islands within the proximal region (−499 to +100) in the cyclin D1 promoter remained unmethylated in both treated and control cells.

3.6. Transcriptional repression of p21 (Waf1/Cip1) by H3K27me3 repressive mark and DNA methylation at the proximal promoter

To analyse the critical role of repressive marks, like H3K27me3 and H2AK119Ub, which may enrich within the p21 promoter to lead p21 transcription inactivation, we used the specific inhibitor of EZH2 (GSK343) or BMI1/PRC1 inhibitor (PRT4165) with or without AFB_1 and checked the expression of p21 in HaCaT cells. We assessed the protein abundance of H3K27me3 and H2AK119Ub (activity product of polycomb proteins) along with p21 and cyclin D1 expression. The results revealed a significant induction of 1.3 fold in p21 expression in presence of polycomb protein inhibitors, GSK343 or PRT4165 (Fig. 4A, B) and an evident reduction in the H3K27me3 and H2AK119Ub levels which were augmented approximately by 2.5 and 3.8 fold ($p < 0.001$) respectively in presence of AFB_1 alone. On the contrary, we did not find any changes in cyclin D1 expression with GSK343 and PRT4165. However, an increase in protein abundance of cyclin D1 approximately by 3.5 and 3 fold was observed when exposed to AFB_1 alone or in combination with both inhibitors respectively (Fig. 4A, B).

To further elucidate the underlying mechanism we mapped the DNMT3a promoter using the MatInspector tool and predicted the potential transcription factor binding sites (TFBS) within the proximal promoter (Fig. 4C). Results showed consensus DNA binding sites for three transcription factors namely Sp1, E2F1, and p53 within −500 bp with respect to the transcription start site (TSS). Similarly, a noticeable alteration in the protein expression of the Sp1, E2F1 and p53 was observed post 24 h of exposure to varying concentrations of AFB_1 in HaCaT cells. The expression of Sp1 and E2F1 increased by ~5.5 and ~4.5 fold independently, while the expression of p53 almost declined with exposure to 1000 nM dose of AFB_1 (Fig. 4D, E). As shown in the Fig. 4F enrichment of transcription factor E2F1 and Sp1 significantly increased at the proximal promoter region of DMNT3a promoter (−406 to −253 and −174 to +17). Next, we analysed the interaction between DNMTs and H3K27me3 or H2AK119Ub upon exposure of HaCaT cells to AFB_1, and more interestingly, an increased interaction between DNMTs and H3K27me3 or H2AK119Ub was confirmed by the immunoprecipitation analysis (Fig. 4G). Further the chromatin immunoprecipitation in HaCaT cells using H3K27me3 and DNMT3a antibodies followed by qPCR at four different regions in the p21 proximal promoter (−594 to −17) validated the enrichment of H3K27me3 repressive mark and recruitment of DNMT3a (Fig. 4H, I). As shown in the Fig. 4H and I, we observed an increased in the enrichment of H3K27me3 and DNMT3a within the p21 promoter with a maximum enrichment towards the vicinity of TSS region R3 (−306 to −216) and R4 (−119/−17) which correspond the region where increased methylation showed by MSP (Fig. 3I, J).

3.7. AFB_1 exposure to Oregon R

The insignificant variation in the optical density (Fig. 5A) in AFB_1 treated media compared to the control in the feeding assay confirmed that the food intake by the flies was not affected by the AFB_1 treatment. The above result substantiated that AFB_1 is not an anti-feedant for *Oregon R* larvae. The LC_{50} concentration was determined by rearing flies in standard wheat cream agar medium containing varying concentrations of AFB_1 as described in materials and methods. Based on the dose responsive curve, the LC_{50} value was calculated as 4.42714 μM (Fig. 5B). Further experiments were carried out using sub lethal concentrations of AFB_1. The larvae consumed the lower concentrations of AFB_1 containing media and then emerged as adult flies after pupation was monitored. The number of pupae developed and the number of adult flies emerged was decreased at higher concentrations compared to that of lower concentrations of AFB_1 (Fig. 5B). At higher concentrations, larvae were less likely to consume the AFB_1 treated food as was evident from the intact surface of the solidified wheat cream agar medium.

3.8. Effect of AFB_1 on the climbing activity of Oregon R at lower doses

The locomotory efficiency of the flies were evaluated upon the treatment with either single or multiple exposures at different doses (0.75 and 1.5 μM) of AFB_1 and it did not show noteworthy locomotory deficits (Fig. 5C). This inferred that AFB_1 does not affect the locomotory function in both males and females at lower doses.

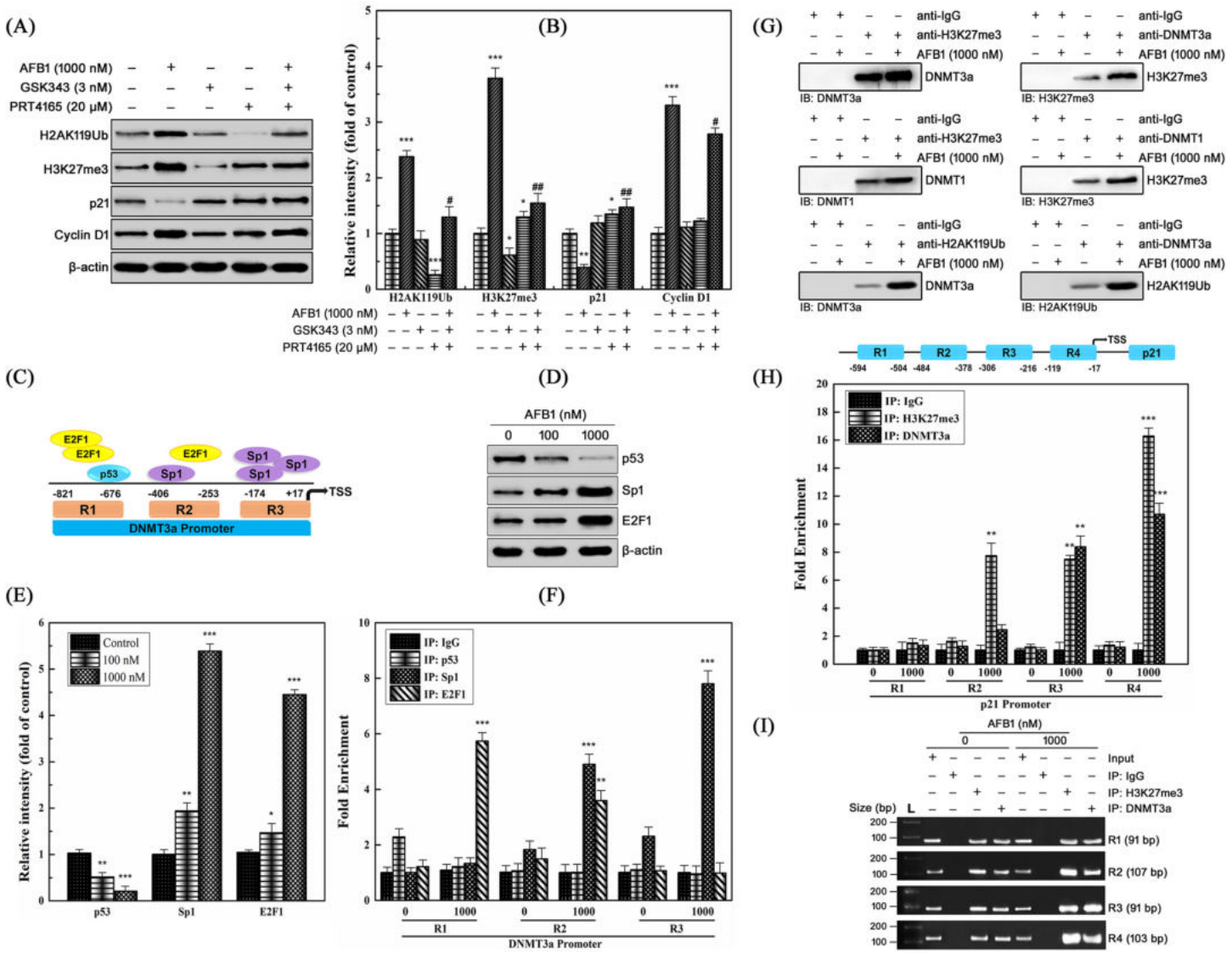

Fig. 4. AFB_1 mediated transcriptional inactivation of p21 in HaCaT cells. **(A)** Cells were incubated with 3 nM of EZH2 inhibitor (GSK343), 20 μM of PRC1 inhibitor (PRT4165), or 1000 nM AFB_1 for 24 h. After treatment, cellular extracts were prepared and total protein (20 microgram) was subjected to immunoblot analysis to detect p21, cyclin D1, H2AK119Ub and H3K27me3 protein level. The β-actin served as the loading control. Cells grown at 0.1% (*v*/*v*) of DMSO were used as an internal control. **(B, E)** The graph represents fold intensities of band related with the control. **(C)** Schematic representation of the regions in the DNMT3a promoter having a consensus sequence for binding of transcription factor p53, E2F1, and Sp1. **(D)** The cells were pre-treated with indicated concentrations of AFB_1 for 24 h followed by loading of total protein (20 microgram) on a polyacrylamide gel for immunoblot analysis to detect the protein level of Sp1, E2F1 and p53. The β-actin served as the loading control. Cells grown at 0.1% (*v*/*v*) of DMSO were used as an internal control. **(F)** Fold enrichment of Sp1, E2F1 and p53 within the selected regions of the DNMT3a promoter. In brief, the cells were incubated with AFB_1 at 1000 nM concentration and post 24 h of exposure, ChIP assay was performed with the help of ChIP grade antibodies or IgG (mock). **(G)** AFB_1 induced DNMT3a-H3K27me3, DNMT1- H3K27me3, and DNMT3a-H2AK119Ub protein-protein interaction. Cells were treated with 1000 nM of AFB_1 for 24 h. The cell lysate was pre-cleared with protein A agarose beads and thereafter immunoprecipitation was performed with either anti-IgG (mock) or anti-DNMT3a or anti-DNMT1 or anti-H3K27me3 or anti-H2AK119Ub antibodies. **(H)** Schematic representation of the four regions in the p21 promoter analysed for H3K27me3 and DNMT3a enrichment *via* ChIP. Fold enrichment for H3K27me3 and DNMT3a within the selected regions of the p21 proximal promoter. The cells were incubated with 1000 nM AFB_1 and post 24 h of exposure, ChIP assay was performed with the help of ChIP grade antibodies or IgG (mock). **(I)** The amplified DNA in qPCR was analysed on 1% agarose gel by electrophoresis. The data statistically represents a mean ± S.D. of triplicates which provided similar results. The statistically significant differences at $p < 0.05$, $p < 0.01$ and $p < 0.001$ level denoted as *, ** and *** respectively against control group, whereas # and ## indicate significant differences at $p < 0.05$ and $p < 0.01$ level *versus* 1000 nM AFB_1.

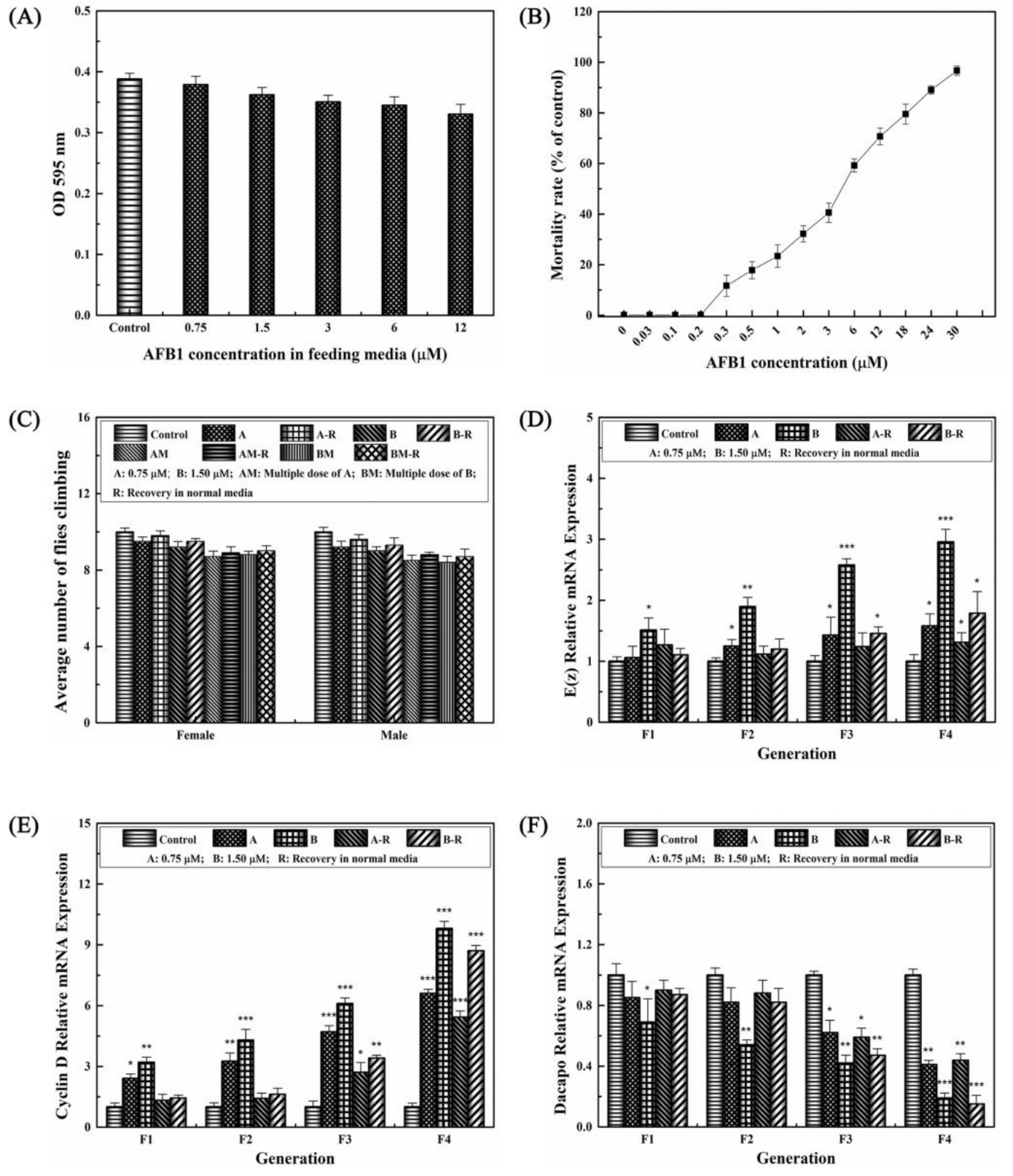

Fig. 5. Effect of AFB_1 on survival ability and expression of epigenetic regulators in *Oregon R*. **(A)** Feeding assay to analyse the food intake in third instar larvae (72 ± 2 h) reared in indicated concentrations of AFB_1 incorporated media. The optical density was measured at 595 nm as an estimate of food consumption. **(B)** Flies were reared in standard wheat cream agar medium containing indicated concentrations of AFB_1. LC_{50} was calculated based on the mortality rate. **(C)** The locomotor performance of male and female flies evaluated *via* negative geotaxis behaviour analysing the climbing behaviour of flies. **(D, E, F)** Dose dependent gene expression of E(z), cyclin D, and Dacapo in *Oregon R*. Flies were reared in 0, 0.75, and 1.5 μM of AFB_1 containing media up to the fourth generation. After exposure to AFB_1 in each generation, the flies were allowed to recover in normal feeding media. Total RNA was isolated and used for E(z), Cyclin D, and Dacapo mRNA using qPCR as described previously. Flies reared in DMSO containing media were served as control. The data statistically represents a mean $\pm$ S.D. of triplicates which provided similar results. The statistically significant difference at $p < 0.05$, $p < 0.01$ and $p < 0.001$ level denoted as *, ** and *** respectively against control group.

3.9. AFB_1 mediated expression of prominent epigenetic regulators

The AFB_1 mediated expression of analogous epigenetic regulators polycomb protein EZH2 analogue E(z), cyclin D1 analogue cyclin D, and p21 analogue Dacapo in *Drosophila*, were analysed followed by the feeding of flies with media containing 0.75 and 1.5 μM of AFB_1. The expression of cyclin D, E(z), and Dacapo was altered in a dose dependent manner with a substantial upsurge in the expression of cyclin D and E(z) with a decrease in the Dacapo, until the fourth generation (Fig. 5D, E, F). The expression of each target was analysed, after flies were allowed to recover from the effects of AFB_1 treatment for one generation after the other. The results demonstrated that the AFB_1 mediated increment in the expression of cyclin D, E(z) and decrease in the expression of Dacapo recovered to certain extent when the flies were allowed to recover in a toxin free media. Furthermore, potency of recovery regressed when the flies were exposed again to the AFB_1 in the subsequent generations (Fig. 5D, E, F) which leads to the upsurge in the expression of targets and suggested the epigenetic memory.

4. Discussion

In the event of development, human population come across to its environment flourished with an effective and vibrant milieu, proficient enough to trigger changes resulting in either the activation or silencing of genes. Exposure to environmental factors like toxic chemicals, pharmaceutical, stress, diet are capable to bring about the negative or positive epigenetic modulations with enduring effects on metabolism, development, and health of the individual. It is evident that at low concentration AFB_1 ensues hyperproliferation that results in the divergence from the regular signaling pathways (Ghufran et al., 2016; Soni et al., 2018; Ghufran et al., 2019). The present study elaborated the mode of action of AFB_1 in cells, to understand the possible mechanisms responsible for the onset of alterations in the epigenetic processes. The BrdU incorporation and Ki67 gene expression analysis exemplified the effect of AFB_1 on cell proliferation as BrdU incorporation and expression of Ki67, are demonstrated index for proliferation (Matatall et al., 2018; Miller et al., 2018). It is evident that the lower concentrations of mycotoxins like AFB_1 and zearalenone, ensued in the cell proliferation and malignancy of MCF-7 cells (Yip et al., 2017). Ki67 is strictly associated with the proliferation growth and migration of malignant cells and is a promising molecular target in the diagnosis of cancer (Miller et al., 2018). The low expression of Ki67 significantly reduced the migration and proliferation of the breast cancer cells (Yuan et al., 2016). The increased transcription of Ki-67 and uptake of BrdU by L-132 and HaCaT cells provided substantial evidence of cellular proliferation at very low concentrations.

The PI3K/Akt/mTOR pathway is a key signaling pathway mainly responsible for regulating the growth, metabolism, and survival (Matsuoka and Yashiro, 2014). To investigate, the AFB_1 mediated intracellular signaling pathways and its downstream cellular effects the PathScan® Intracellular Signaling Array analysis was performed. The results demonstrated that AFB_1 triggered the activation of Akt by its phosphorylation at Serine 473, which in turn phosphorylates multiple downstream substrates that regulate the vital cellular functions. The mTOR is an essential downstream target (Manning and Toker, 2017) of Akt where it can directly phosphorylate at Ser2448, which in turn activates mTORC1 (Chen et al., 2016a). Upon AFB_1 exposure, other than the Akt phosphorylation, mTOR, ERK1/2, Bad, PRAS40 and GSK3β phosphorylation were also elevated with declined phosphorylation of p38. The decreased p38 phosphorylation is in accordance with our previous report (Ghufran et al., 2019). The Bad, a pro-apoptotic protein in the absence of growth/survival factors remained associated with anti-apoptotic Bcl-2/Bcl-xl proteins that hamper the anti-apoptotic potential (Song et al., 2005). The Akt-mediated Bad phosphorylation at Ser112 leads to the inhibition of its pro-apoptotic potential, when it get phosphorylated cannot bind to prosurvival Bcl-2/Bcl-xl (Song et al., 2005; Manning and Cantley, 2007). In the present study Bad, which is believed to be one of the direct targets of Akt for transmitting survival signals was phosphorylated at S112 upon AFB_1 treatment suggested the AFB_1 mediated transmission of survival signal. The phosphorylation of GSK-3 isoforms by Akt/PKB on an extremely conserved N-terminal site (GSK3β-S9), revealed the inactivation of the kinase (Manning and Toker, 2017). The GSK3 and Akt/PKB elicits a grid that categorically regulates G1/S cell cycle progression *via* deactivation of GSK3-β, which pertains to an increase in the expression of cyclin D1 (Maurer et al., 2014). Another mycotoxin Fumonisin B1 exposure in hepatocytes, resulted in the activation of Akt which later enhance the cell survival, with inhibition of GSK-3β and post-translational stabilization of cyclin D1 that disrupted the cell cycle at G(1)/S restriction point (Ramljak et al., 2000). Similarly, in lymphoblastoid cell lines (LCLs), treatment with 50 μM of AFB_1 demonstrated a significant increase in phosphorylation at serine 9 of GSK3β (Accardi et al., 2015). Maurya and Trigun (2017) have validated the Akt dependent cell growth signaling mechanisms in AFB_1 induced hepatocellular carcinoma (Maurya and Trigun, 2017). The Akt and mTORC1 mediated phosphorylation of PRAS40 interrupts the binding between mTORC1 and PRAS40 thereby relieving the inhibitory control of PRAS40 on mTORC1 (Wang et al., 2012). As a result, the phosphorylated, mTORC1-dissociated PRAS40 serves its peculiar prosurvival function by promoting protein synthesis, cell survival, and tumorigenesis (Wang et al., 2012; Havel et al., 2015). Elevated phosphorylation of PRAS40 at Thr 246 residue phosphorylation has been reported in numerous cancer cell lines in addition to meningioma's and malignant melanomas (Wiza et al., 2012). Our study also affirmed the AFB_1 mediated Akt activation and PRAS40 phosphorylation. The validation of array results evidenced that AFB_1 treatment significantly enhanced the phosphorylation of Akt, mTOR, and Bad, which was further increased in presence of Akt activator Sc-79 in conversely AFB_1 mediated phosphorylation of Akt diminished in presence of its inhibitor Triciribine. These results eventually demonstrated the proliferative role of AFB_1 which may pave its way towards tumorigenesis.

AFB_1 has a role in cell proliferation and pro survival signaling as it may affect the cell cycle. The level of cyclins and cyclin-dependent kinase inhibitor (CKI) post treatment with doses of AFB_1 was observed with maximum expression at 1000 nM. The members of the Cip/Kip family proteins (p27Kip1/Cdkn1b, p57Kip2/Cdkn1c, p21Cip1/Waf1/Cdkn1a) interacts with cyclin A-, D-, E-, and B-CDK complexes that constrain their activity leading to repression of cellular senescence and increased tumorigenicity (Szymonowicz et al., 2018; Bisteau et al., 2013). An increased expression of cyclin D1 in the early G1 phase is mediated by the cell cycle inhibitor p21, as it consents the nuclear position of complexes of Cdk4/cyclin D and alleviates the formation without hindering their activity. A decrease in the p21 expression level is initiated during the G1/S transition following its sequestration by Cdk4–6/cyclin D complexes and thus directs activation of Cdk2/cyclin E (Bisteau et al., 2013). The increment in the expression of cyclin D1 protein and concurrent reduction in the expression level of cell cycle inhibitor p21 by AFB_1 in HaCaT and L-132 cells suggested its role in cell cycle. Transcriptional suppression by promoter directed hypermethylation serves to be one of the most explored mechanisms in carcinogenesis. The p21 promoter analysis was carried to access the reason for the distinctive expression of cyclin D1 and p21, and it revealed that an assembly of the high density of theoretically methylatable CpG dinucleotides neighbouring transcription start site (TSS), affirmed our hypothesis that the transcriptional fate of p21 can be regulated by methylation. The reduced expression of p21 on post exposure to AFB_1 seems to be the consequence of hypermethylation of CpG islands (CGIs) in the p21 promoter. As previously demonstrated AFB_1 leads to the overexpression of DNMTs (Soni et al., 2018) and was obliged to the methylation of p21 promoter. Typically, methylated CGIs in a promoter repress the transcriptional activation and on the contrary, unmethylated CGIs permit the initiation of transcription (Qimuge et al., 2019). This is in synchronisation with our results where AFB_1 mediate the increase in methylation of CpGs in p21 promoter that resulted in the reduced expression. Since

the CpGs in cyclin D1 promoter remains unmethylated as shown in MSP results, it remained transcriptionally active and enhanced the expression of cyclin D1. Hypermethylation of p21 promoter is also reported to be involved in the pathogenesis of malignancies such as lymphoma and acute lymphoblastic leukemia (Soltanpour et al., 2013). In adult T-cell leukemia/lymphoma (ATLL) cells, reduced p21 expression, and hypermethylation of p21 promoter possibly lead ATLL leukemogenesis (Watanabe et al., 2010).

Reports suggested that an epigenetic modifier has a vital role in the transcriptional inactivation of p21 in multiple models (Zhao et al., 2013). For instance, melanoma cells substantiate the effects of EZH2 on senescence and cell cycle *via* EZH2-dependent regulation of p21 (Fan et al., 2011). In numerous cancers like breast, bladder, prostate, lung, oral squamous cell carcinoma, and colorectal cancer the overexpression of BMI-1 and EZH2 with poor diagnosis besides higher oncogenic potential was reported (Balasubramanian et al., 2012). Studies have also revealed that BMI1, EZH2, and DNMTs collaborate to suppress gene expression of target proteins either by modulation of histones or DNA methylation (So et al., 2011). Since the critical repressive marks, like H3K27me3 and H2AK119Ub, were found to be significantly enriched due to AFB_1 mediated polycomb protein expression (Soni et al., 2018), we rationalized that these repressive marks may enrich within the p21 promoter to cause its suppression. The pharmacological inhibitors of EZH2 (GSK343) or PRC1 (PRT4165) strongly suppressed p21 which validated the EZH2 mediated silencing of p21 with concurrent reduction in repressive marks H3K27me3 and H2AK119Ub. Likewise, Itahana et al. also revealed the H3K27me3 mediated epigenetic silencing of p21 where p21 expression was elevated with reduced H3K27me3 mark in the presence of DZNep, a pharmacological inhibitor of PRC2 (Itahana et al., 2016). The enrichment of the H3K27me3 repressive mark at the p21 proximal promoter substantiated the transcriptional suppression of p21 mediated by EZH2.

AFB_1 suppresses the p21 and upregulates the cyclin D1 and EZH2 selectively suppresses the p21 without affecting the cyclin D1 expression. During tumorigenesis, the two *de novo* methyltransferases, DNMT3a and DNMT3b primarily imprint methylation marks in site specific hypermethylation of cancer-associated genes (Hervouet et al., 2009). It is reported that AFB_1 upregulates the expression of maintenance methyltransferase DNMT3a (Soni et al., 2018). To delineate the underlying mechanism of up regulation of DNMT3a, we mapped the DNMT3a promoter for transcription factor binding sites. The promoter harbour the binding sites for transcription factors p53, Sp1 and E2F1 with an enhanced enrichment of Sp1 and E2F1 mediated by AFB_1 in the proximal region of the DNMT3a promoter whereas p53 level was reduced. The genome-wide analysis of histone modification like H3K27me3 revealed that it may serve as the docking site for the recruitment of DNMTs and thus involved in controlling DNA methylation to particular chromatin regions (Deplus et al., 2014). Interestingly, AFB_1 enhanced the interaction between DNMT3a and H3K27me3 in HaCaT cells, and moreover, DNMT3a and H3K27me3 mark enriched at the p21 promoter with a more enrichment vicinal to TSS region R3 (−306 to −216) and R4 (−119/−17) which adds for the methylation of proximal promoter that leads to repression of p21. Similar phenomenon was reported where DNMT inhibition induced the expression of p21 trailed by cell cycle arrest and decreased proliferation (So et al., 2011).

After deciphering the *in vitro* role of AFB_1 in regulation of epigenetic scaffold, it prompted us to investigate the AFB_1 mediated epigenetic alterations in *Drosophila melanogaster*. *D. melanogaster*, has a high scientific history in biological research contributed much towards a better understanding of evolutionary concepts, developmental biology, and toxicology as well as epigenetic regulation (Merinas-Amo et al., 2019). Moreover, a high degree of homology among the mammalian and *Drosophila* genome (Yamamoto et al., 2014) makes the fly an appropriate model system to dissect the insights about epigenetic modifications associated with the onset of diseases like cancer. *D. melanogaster* has frequently offered a significant role in interpreting the molecular basis of diseases as it provides the initial indications about the mode of action and mechanisms behind the regulation of human cancer-related proteins (Gonzalez, 2013). The flies fed on lower doses of AFB_1 did not show any deleterious developmental effects. But a higher concentration of AFB1 has led to a decline in the overall count of flies pupated or emerged. However, at extremely higher concentrations of AFB_1, the flies showed signs of developmental retardation. The higher pre adult mortality and prolonged developmental time from larva to adult was observed as the concentration of AFB_1 is increased. The observed reduction in pre adult survivorship could possibly be due to the inability of flies for detoxification. The accumulation of AFB_1 at higher doses, within the flies might have induced deleterious effects on larva probably have reduced its survival potential that might have decreased the rate of larvae transforming to pupae (Mitchell et al., 2015; Mathew and Krishnamurthy, 2018). Drott *et al*, reported that eggs were pupated but subsequently no adults have emerged at 3000 and 4000 ppb dose of AFB_1 (Drott et al., 2017) which supports our observation. The concentration range of AFB_1 used in the experiments was very much close to the human exposure range where the expression pattern of vital epigenetic regulators was addressed.

The basal activity level of the flies can be interpreted by keeping account of non-strenuous activity through assessing their spontaneous locomotion with the response to AFB_1. Since the flies have to work against gravity to climb to the top of the climbing apparatus, vertical climbing serves as a valuation of *D. melanogaster's* ability to finish a vigorous activity, providing insight into its level of physical fitness (Lee et al., 2010). The analysis of the expression pattern of *Drosophila* cell cycle regulators Dacapo and cyclin D along with the polycomb protein E(z) here served imperative roles as epigenetics regulators. These regulators escort the alterations in chromatin remodeling or histone modifying complexes which pave the way towards the survival of the organism. *Drosophila* possess a single Cyclin D that along with Cdk4 subunit, forms an active kinase complex leading to prompt divisions with normal cell cycle and improved rate of cell growth. However, its overexpression plays a prominent role in cell growth in the development of flies with a shortened cycle (Datar et al., 2006). Dacapo (Dap) is a homologue of mammalian p21 family which encodes an inhibitor molecule similar to the Cip/Kip inhibitors of vertebrate that functionally restrain the activity of cyclin *E*-CDK2 complex (Swanson et al., 2015). Enhancer of zeste E(z) protein exerts histone methyltransferase activity specific for lysine 27 residue on histone H3 (H3K27) which plays a crucial role in gene silencing as E(z) carry out remodeling of chromatin thus alters gene expression (Solovev et al., 2018). Our findings demonstrated that the mRNA abundance of cyclin D and E (z) increased significantly with a decline in the Dacapo expression when the flies were fed with wheat cream agar media containing AFB_1. The generation wise study revealed a consistent increase in the mRNA abundance of E(z) and cyclin D with a consistent decrease in mRNA expression of Dacapo at F4 generation. In addition, after each generation a decrease in the rate of recovery of initial expression patterns was observed when allowed to recover in normal media without AFB_1. The consistence in maintaining the expression of these regulators imparted by AFB_1 exposure with a decreased rate of recovery suggested a multigenerational epigenetic memory in *Oregon R* flies.

Our results suggested the ability of AFB_1 to modify the expression and functions of polycomb proteins and the consequent enhancement in chromatin repressive marks eventually silencing the gene. As emerging proofs have firmly associated the tumerogenic role of EZH2 and BMI-1 with the escalated proliferation of cancer cells; present data, suggested the fact that AFB_1 mediated epigenetic transcriptional inactivation of p21 *via* EZH2 activity could be a possible mechanism of the health inferences in exposed individuals. To the best of our knowledge, it is first time that an integrative approach (*in vivo* and *in vitro*) has been performed to understand the basic mechanisms behind concentration dependent and generation wise AFB_1 mediated expression of epigenetic regulators in cell lines and the model system *D. melanogaster* simultaneously. The study proposes first-hand perspectives on the AFB_1

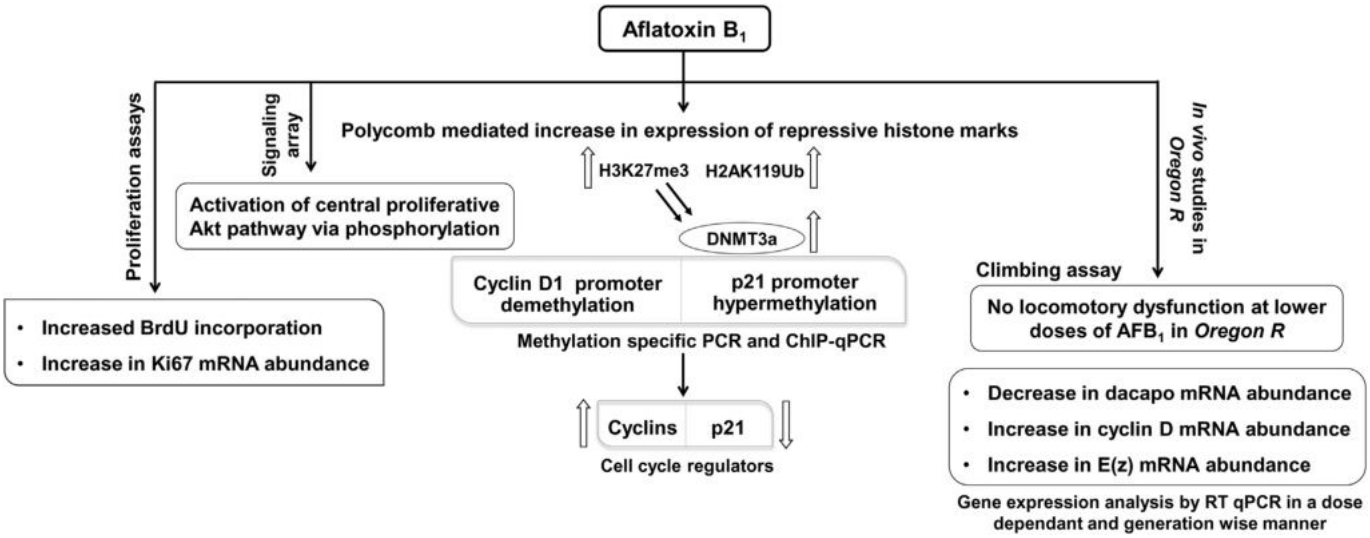

Fig. 6. Schematic diagram representing the possible influential role of AFB_1 on cell proliferation and p21 silencing. The findings of the present study indicated an increase in cellular proliferation *via* activation of Akt pathway. The formation of repressive histone marks further caused the enrichment of DNMT3a at the p21 promoter and enhanced its methylation. Overall these modifications eventually lead to the deregulation of cell cycle regulator molecules. *In vivo* study illustrated that AFB_1 altered the expression of E(z), Cyclin D and Dacapo in *Oregon R*. The proposed mechanism establishes the potential of AFB_1 and the interconnection between different pathways and epigenetic modifications leading to cellular proliferation and might end up in the process of tumorigenesis.

mediated expression of vital epigenetic regulators in a *Drosophila* model. Moreover, in-depth supplementary research on the biological as well as epigenetic aspects of AFB_1 mediated alterations in advanced model systems is necessary to unveil and conceptualize the intricate grid of key signaling molecules and its epigenetic memory.

5. Conclusion

In summary, our findings demonstrated that AFB_1 activated the Akt pathway resulting in transmission of survival signals *via* its downstream target molecules (Fig. 6). The reduced expression of p21 further suggested the altered cellular functions and enhanced tumorigenicity caused by AFB_1. Besides, the use of EZH2 inhibitors posing favorable anti-cancer activity may enhance the effectiveness of several existing anticancer drugs. The altered expression of core epigenetic regulators in *D. melanogaster* indeed serves as a primary screening platform to provide insights regarding the complex regulatory network. Scientifically engineered *D. melanogaster* strains can be useful to summarize the crucial features of varied cancer types paving the way towards new frontiers in biomedical research which may further facilitate the development of platforms for therapeutic drug discovery in the future.

Supplementary data to this article can be found online at https://doi.org/10.1016/j.scitotenv.2020.143175.

CRediT authorship contribution statement

PS: designed and performed *in vivo* and *in vitro* experiments, analysed and interpreted the results and wrote the manuscript; MSG: performed *in vitro* experiments, performed statistical data analysis and designed the figures; SO: helped with *in vivo* experiments; GHP: generously provided the fly stocks and lab space for carrying out the *in vivo* work, helped in troubleshooting; GRD: provided the lab space helped in troubleshooting in *in vivo* work analysis; SRK: conceptualized, designed the experiments, interpreted the data, supervised the entire work and edited the manuscript.

Declaration of competing interest

All authors declare that there is no conflict of interest.

Acknowledgments

The authors are grateful to the Science and Engineering Research Board (SERB) Govt. of India for financial support (Grant No EEQ/2016/000251) and Kerala State Council for Science, Technology and Environment (KSCSTE), Govt. of Kerala for research fellowship to PS.

References

Accardi, R., Gruffat, H., Sirand, C., Fusil, F., Gheit, T., Hernandez-Vargas, H., Le Calvez-Kelm, F., Traverse-Glehen, A., Cosset, F.L., Manet, E., Wild, C.P., Tommasino, M., 2015. The mycotoxin aflatoxin B_1 stimulates Epstein-Barr virus-induced B-cell transformation in in vitro and in vivo experimental models. Carcinogenesis 36 (11), 1440–1451. https://doi.org/10.1093/carcin/bgv142.

Akizu, N., García, M.A., Estarás, C., Fueyo, R., Badosa, C., de la Cruz, X., Martínez-Balbás, M.A., 2016. EZH2 regulates neuroepithelium structure and neuroblast proliferation by repressing p21. Open Biol. 6 (4), 150227. https://doi.org/10.1098/rsob.150227.

Aloia, L., Di Stefano, B., Di Croce, L., 2013. Polycomb complexes in stem cells and embryonic development. Development 140 (12), 2525–2534. https://doi.org/10.1242/dev.091553.

Balasubramanian, S., Kanade, S., Han, B., Eckert, R.L., 2012. A proteasome inhibitor-stimulated Nrf1 protein-dependent compensatory increase in proteasome subunit gene expression reduces polycomb group protein level. J. Biol. Chem. 287, 36179–36189. https://doi.org/10.1074/jbc.M112.359281.

Bartholomew, N., Burdett, J.M., VandenBrooks, J.M., Quinlan, M.C., Call, G.B., 2015. Impaired climbing and flight behaviour in *Drosophila melanogaster* following carbon dioxide anaesthesia. Sci. Rep. 5, 15298. https://doi.org/10.1038/srep15298.

Bbosa, G.S., Kitya, D., Odda, J., Ogwal-okeng, J., 2013. Aflatoxins metabolism, effects on epigenetic mechanisms and their role in carcinogenesis. Sci. Res. 5, 14–34. https://doi.org/10.4236/health.2013.510A1003.

Bisteau, X., Paternot, S., Colleoni, B., Ecker, K., Coulonval, K., De Groote, P., Declercq, W., Hengst, L., Roger, P.P., 2013. CDK4 T172 phosphorylation is central in a CDK7-dependent bidirectional CDK4/CDK2 interplay mediated by p21 phosphorylation at the restriction point. PLoS Genet. 9 (5), e1003546. https://doi.org/10.1371/journal.pgen.1003546.

Bradford, M.M., 1976. A rapid and sensitive method for the quantitation of microgram quantities of protein utilizing the principle of protein-dye binding. Anal. Biochem. 72, 248–254. https://doi.org/10.1006/abio.1976.9999.

Chappell, G., Pogribny, I.P., Guyton, K.Z., Rusyn, I., 2016. Epigenetic alterations induced by genotoxic occupational and environmental human chemical carcinogens: a systematic literature review. Mutat. Res. Rev. Mutat. Res. 768, 27–45. https://doi.org/10.1016/j.mrrev.2016.03.004.

Chen, B., Li, D., Li, M., Li, S., Peng, K., Shi, X., Zhou, L., Zhang, P., Xu, Z., Yin, H., Wang, Y., Zhao, X., Zhu, Q., 2016a. Induction of mitochondria-mediated apoptosis and PI3K/Akt/mTOR-mediated autophagy by aflatoxin B_2 in hepatocytes of broilers. Oncotarget 7 (51), 84989–84998. https://doi.org/10.18632/oncotarget.13356.

Chen, Y., Pan, K., Wang, P., Cao, Z., Wang, W., Wang, S., Hu, N., Xue, J., Li, H., Jiang, W., Li, G., Zhang, X., 2016b. HBP1-mediated regulation of p21 protein through the Mdm2/p53 and TCF4/EZH2 pathways and its impact on cell senescence and tumorigenesis. J. Biol. Chem. 291 (24), 12688–12705. https://doi.org/10.1074/jbc.M116.714147.

Dai, Y., Huang, K., Zhang, B., Zhu, L., Xu, W., 2017. Aflatoxin B_1-induced epigenetic alterations: an overview. Food Chem. Toxicol. 109 (Pt1), 683–689. https://doi.org/10.1016/j.fct.2017.06.034.

Dall'Asta, C., 2016. Mycotoxins and nuclear receptors: a still underexplored issue. Nucl. Recept. Res. 3, 101204. https://doi.org/10.11131/2016/101204.

Datar, S.A., Galloni, M., de la Cruz, A., Marti, M., Edgar, B.A., Frei, C., 2006. Mammalian cyclin D1/Cdk4 complexes induce cell growth in Drosophila. Cell Cycle (Georgetown, Tex.) 5 (6), 647–652.

Delcour, J., 1969. A rapid and efficient method of egg collection. Dros. Inform. Serv. 44, 133–134.

Deplus, R., Denis, H., Putmans, P., Calonne, E., Fourrez, M., Yamamoto, K., Suzuki, A., Fuks, F., 2014. Citrullination of DNMT3A by PADI4 regulates its stability and controls DNA methylation. Nucleic Acids Res. 42 (13), 8285–8296. https://doi.org/10.1093/nar/gku522.

Drott, M.T., Lazzaro, B.P., Brown, D.L., Carbone, I., Milgroom, M.G., 2017. Balancing selection for aflatoxin in *Aspergillus flavus* is maintained through interference competition with, and fungivory by insects. Proc. R. Soc. B 284, 20172408. https://doi.org/10.1098/rspb.2017.2408.

Fan, T., Jiang, S., Chung, N., Alikhan, A., Ni, C., Lee, C.C., Hornyak, T.J., 2011. EZH2-dependent suppression of a cellular senescence phenotype in melanoma cells by inhibition of p21/CDKN1A expression. Mol. Cancer Res. 9 (4), 418–429. https://doi.org/10.1158/1541-7786.MCR-10-0511.

Feinberg, A.P., Koldobskiy, M.A., Göndör, A., 2016. Epigenetic modulators, modifiers and mediators in cancer aetiology and progression. Nat. Rev. Genet. 17 (5), 284–299. https://doi.org/10.1038/nrg.2016.13.

Ghufran, M.S., Soni, P., Kanade, S., 2016. Aflatoxin B_1 induced upregulation of protein arginine methyltransferase 5 in human cell lines. Toxicon 119, 117–121. https://doi.org/10.1016/j.toxicon.2016.05.015.

Ghufran, M.S., Soni, P., Kanade, S., 2019. Aflatoxin-induced upregulation of protein arginine methyltransferase 5 is mediated by protein kinase C and extracellular signal-regulated kinase. Cell Biol. Toxicol. 35 (1), 67–80. https://doi.org/10.1007/s10565-018-9439-8.

Gonzalez, C., 2013. *Drosophila melanogaster*: a model and a tool to investigate malignancy and identify new therapeutics. Nat. Rev. Cancer 13, 172–183. https://doi.org/10.1038/nrc3461.

Havel, J.J., Li, Z., Cheng, D., Peng, J., Fu, H., 2015. Nuclear PRAS40 couples the Akt/mTORC1 signaling axis to the RPL11-HDM2-p53 nucleolar stress response pathway. Oncogene 34 (12), 1487–1498. https://doi.org/10.1038/onc.2014.91.

Herceg, Z., Lambert, M.P., van Veldhoven, K., Demetriou, C., Vineis, P., Smith, M.T., Straif, K., Wild, C.P., 2013. Towards incorporating epigenetic mechanisms into carcinogen identification and evaluation. Carcinogenesis 34 (9), 1955–1967. https://doi.org/10.1093/carcin/bgt212.

Hervouet, E., Vallette, F.M., Cartron, P.F., 2009. Dnmt3/transcription factor interactions as crucial players in targeted DNA methylation. Epigenetics 4 (7), 487–499. https://doi.org/10.4161/epi.4.7.9883.

Itahana, Y., Zhang, J., Göke, J., Vardy, L.A., Han, R., Iwamoto, K., Cukuroglu, E., Robson, P., Pouladi, M.A., Colman, A., Itahana, K., 2016. Histone modifications and p53 binding poise the p21 promoter for activation in human embryonic stem cells. Sci. Rep. 6 (28112), 2016. https://doi.org/10.1038/srep28112.

Laemmli, U.K., 1970. Cleavage of structural proteins during the assembly of the head of bacteriophage T4. Nature 227, 680–685. https://doi.org/10.1038/227680a0.

Lee, K.S., Lee, B.S., Semnani, S., Avanesian, A., Um, C.Y., Jeon, H.J., Seong, K.M., Yu, K., Min, K.J., Jafari, M., 2010. Curcumin extends life span, improves health span, and modulates the expression of age-associated aging genes in *Drosophila melanogaster*. Rejuvenation Res. 13, 561–570. https://doi.org/10.1089/rej.2010.1031.

Manning, B.D., Cantley, L.C., 2007. AKT/PKB signaling: navigating downstream. Cell 129, 1261–1274. https://doi.org/10.1016/j.cell.2007.06.009.

Manning, B.D., Toker, A., 2017. AKT/PKB signaling: navigating the network. Cell 169 (3), 381–405. https://doi.org/10.1016/j.cell.2017.04.001.

Matatall, K.A., Kadmon, C.S., King, K.Y., 2018. Detecting hematopoietic stem cell proliferation using BrdU incorporation. Methods Mol. Biol. 1686, 91–103. https://doi.org/10.1007/978-1-4939-7371-2_7.

Mathew, B.B., Krishnamurthy, N.B., 2018. Assessment of lead toxicity using *Drosophila melanogaster* as a model. J. Clin. Toxicol. 8, 380. https://doi.org/10.4172/2161-0495.1000380.

Matsuoka, T., Yashiro, M., 2014. The role of PI3K/Akt/mTOR signaling in gastric carcinoma. Cancers 6, 1441–1463. https://doi.org/10.3390/cancers6031441.

Maurer, U., Preiss, F., Brauns-Schubert, P., Schlicher, L., Charvet, C., 2014. GSK-3 - at the crossroads of cell death and survival. J. Cell Sci. 127 (Pt 7), 1369–1378. https://doi.org/10.1242/jcs.138057.

Maurya, B.K., Trigun, S.K., 2017. Fisetin attenuates AKT associated growth promoting events in Aflatoxin B_1 induced hepatocellular carcinoma. Anti Cancer Agents Med. Chem. 18 (13), 1885–1891. https://doi.org/10.2174/1871520618666171229223335.

Melone, P.D., Chinnici, J.P., 1986. Selection for increased resistance to aflatoxin B1 toxicity in *Drosophila melanogaster*. J. Invertebr. Pathol. 48 (1), 60–65. https://doi.org/10.1016/0022-2011(86)90143-6.

Merinas-Amo, R., Martínez-Jurado, M., Jurado-Güeto, S., Alonso-Moraga, Á., Merinas-Amo, T., 2019. Biological effects of food coloring in *in vivo* and *in vitro* model systems. Foods 8 (5), 176. https://doi.org/10.3390/foods8050176.

Miller, I., Min, M., Yang, C., Tian, C., Gookin, S., Carter, D., Spencer, S.L., 2018. Ki67 is a graded rather than a binary marker of proliferation versus quiescence. Cell Rep. 24 (5), 1105–1112.e5. https://doi.org/10.1016/j.celrep.2018.06.110.

Mitchell, C.L., Yeager, R.D., Johnson, Z.J., D'Annunzio, S.E., Vogel, K.R., Werner, T., 2015. Long-term resistance of *Drosophila melanogaster* to the mushroom toxin alpha-amanitin. PLoS One 10 (5), e0127569. https://doi.org/10.1371/journal.pone.0127569.

Nelson, J.D., Denisenko, O., Bomsztyk, K., 2006. Protocol for the fast chromatin immunoprecipitation (ChIP) method. Nat. Protoc. 2006;1 (1), 179–185. https://doi.org/10.1038/nprot.2006.27.

Qimuge, N., He, Z., Qin, J., Sun, Y., Wang, X., Yu, T., Dong, W., Yang, G., Pang, W., 2019. Overexpression of DNMT3A promotes proliferation and inhibits differentiation of porcine intramuscular preadipocytes by methylating p21 and PPARg promoters. Gene 696, 54–62. https://doi.org/10.1016/j.gene.2019.02.029.

Ramljak, D., Calvert, R.J., Wiesenfeld, P.W., Diwan, B.A., Catipovic, B., Marasas, W.F., Victor, T.C., Anderson, L.M., Gelderblom, W.C., 2000. A potential mechanism for fumonisin B (1)-mediated hepatocarcinogenesis: cyclin D1 stabilization associated with activation of Akt and inhibition of GSK-3beta activity. Carcinogenesis 21 (8), 1537–1546. https://doi.org/10.1093/carcin/21.5.537.

So, A.Y., Jung, J.W., Lee, S., Kim, H.S., Kang, K.S., 2011. DNA methyltransferase controls stem cell aging by regulating BMI1 and EZH2 through microRNAs. PLoS One 6 (5), e19503. https://doi.org/10.1371/journal.pone.0019503.

Solovev, I., Shaposhnikov, M., Kudryavtseva, A., Moskalev, A., 2018. *Drosophila melanogaster* as a Model for Studying the Epigenetic Basis of Aging. Epigenetics of Aging and Longevity. Edition: 1, Chapter: 14. Translational Epigenetics. 4. Academic Press, Elsevier Inc., pp. 293–307. https://doi.org/10.1016/B978-0-12-811060-7.00014-0.

Soltanpour, M.S., Amirizadeh, N., Zaker, F., Oodi, A., Nikougoftar, M., Kazemi, A., 2013. mRNA expression and promoter DNA methylation status of CDKi p21 and p57 genes in ex vivo expanded CD34 (+) cells following co-culture with mesenchymal stromal cells and growth factors. Hematology 18 (1), 30–38. https://doi.org/10.1179/1607845412Y.0000000030.

Song, G., Ouyang, G., Bao, S., 2005. The activation of Akt/PKB signaling pathway and cell survival. J. Cell. Mol. Med. 9 (1), 59–71. https://doi.org/10.1111/j.1582-4934.2005.tb00337.x.

Soni, P., Ghufran, M.S., Kanade, S., 2018. Aflatoxin B_1 induced multiple epigenetic modulators in human epithelial cell lines. Toxicon 151, 119–128. https://doi.org/10.1016/j.toxicon.2018.07.011.

Stein, R.A., 2012. Epigenetics and environmental exposures. J. Epidemiol. Community Health 66, 8–13. https://doi.org/10.1136/jech.2010.130690.

Swanson, C.I., Meserve, J.H., McCarter, P.C., Thieme, A., Mathew, T., Elston, T.C., Duronio, R.J., 2015. Expression of an S phase-stabilized version of the CDK inhibitor Dacapo can alter endoreplication. Development (Camb.) 142 (24), 4288–4298. https://doi.org/10.1242/dev.115006.

Szymonowicz, K., Oeck, S., Malewicz, N.M., Jendrossek, V., 2018. New insights into protein kinase B/Akt signaling: role of localized Akt activation and compartment-specific target proteins for the cellular radiation response. Cancers (Basel) 10 (3). https://doi.org/10.3390/cancers10030078 pii: E78.

Taylor, M.J., Tuxworth, R.I., 2019. Continuous tracking of startled *Drosophila* as an alternative to the negative geotaxis climbing assay. J. Neurogenet. 33 (3), 190–198. https://doi.org/10.1080/01677063.2019.1634065.

Wang, H., Zhang, Q., Wen, Q., Zheng, Y., Lazarovici, P., Jiang, H., Lin, J., Zheng, W., 2012. Proline-rich Akt substrate of 40 kDa (PRAS40): a novel downstream target of PI3k/Akt signaling pathway. Cell. Signal. 24 (1), 17–24. https://doi.org/10.1016/j.cellsig.2011.08.010.

Watanabe, M., Nakahata, S., Hamasaki, M., Saito, Y., Kawano, Y., Hidaka, T., Yamashita, K., Umeki, K., Taki, T., Taniwaki, M., Okayama, A., Morishita, K., 2010. Downregulation of CDKN1A in adult T-cell leukemia/lymphoma despite overexpression of CDKN1A in human T-lymphotropic virus 1-infected cell lines. J. Virol. 84 (14), 6966–6977. https://doi.org/10.1128/JVI.00073-10.

Wiza, C., Nascimento, E.B., Ouwens, D.M., 2012. Role of PRAS40 in Akt and mTOR signaling in health and disease. Am. J. Physiol. Endocrinol. Metab. 302 (12), E1453–E1460. https://doi.org/10.1152/ajpendo.00660.2011.

Yamamoto, S., Jaiswal, M., Charng, W.L., Gambin, T., Karaca, E., Mirzaa, G., Wiszniewski, W., Sandoval, H., Haelterman, N.A., Xiong, B., Zhang, K., Bayat, V., David, G., Li, T., Chen, K., Gala, U., Harel, T., Pehlivan, D., Penney, S., Vissers, L.E.L.M., de Ligt, J., Jhangiani, S.N., Xie, Y., Tsang, S.H., Parman, Y., Sivaci, M., Battaloglu, E., Muzny, D., Wan, Y.W., Liu, Z., Lin-Moore, A.T., Clark, R.D., Curry, C.J., Link, N., Schulze, K.L., Boerwinkle, E., Dobyns, W.B., Allikmets, R., Gibbs, R.A., Chen, R., Lupski, J.R., Wangler, M.F., Bellen, H.J., 2014. A *drosophila* genetic resource of mutants to study mechanisms underlying human genetic diseases. Cell. 159 (1), 200–214. https://doi.org/10.1016/j.cell.2014.09.0002.

Yip, K.Y., Wan, M., Wong, A., Korach, K.S., El-Nezami, H., 2017. Combined low-dose zearalenone and aflatoxin B_1 on cell growth and cell-cycle progression in breast cancer MCF-7 cells. Toxicol. Lett. 281, 139–151. https://doi.org/10.1016/j.toxlet.2017.09.022.

Yuan, P., Xu, B., Wang, C., Zhang, C., Sun, M., Yuan, L., 2016. Ki-67 expression in luminal type breast cancer and its association with the clinicopathology of the cancer. Oncol. Lett. 11 (3), 2101–2105. https://doi.org/10.3892/ol.2016.4199.

Zhao, Y., Guo, J., Zhang, X., Zhang, Z., Gu, S., Fei, C., Li, X., Chang, C., 2013. Downregulation of p21 in myelodysplastic syndrome is associated with p73 promoter hypermethylation and indicates poor prognosis. Am. J. Clin. Pathol. 140 (6), 819–827. https://doi.org/10.1309/AJCPZ5E6IWPWSZXE.